

Mu2e Calibration: Electron Spectrometer and Magnetic Fields

John Alsterda^a, Grace Bluhm^{a,c}, George Gollin^{a,1}, Tim He^a, Guangyong Koh^a, Matthew McHugh^a, Daniel Pershey^{a,b}

^aDepartment of Physics, University of Illinois at Urbana-Champaign

^bDepartment of Physics, Harvard University

^cDepartment of Physics, University of Wisconsin-Whitewater

August 7, 2009

Abstract

We describe a magnetic spectrometer that is part of a proposed calibration beam for the Mu2e experiment. The spectrometer is configured to produce electrons of precisely known energy. We find that the spectrometer can select electrons within about 10 keV of a desired energy of 105 MeV, a reduction from the 100 keV RMS width expected for a beam from an upgraded AØ photoinjector.

Simulated data were collected by injecting electrons into the spectrometer with Gaussian distributions of possible parameters. Results and conclusions about the spectrometer's effectiveness were drawn from analysis of histograms containing information about the trajectories of the simulated electrons.

Introduction

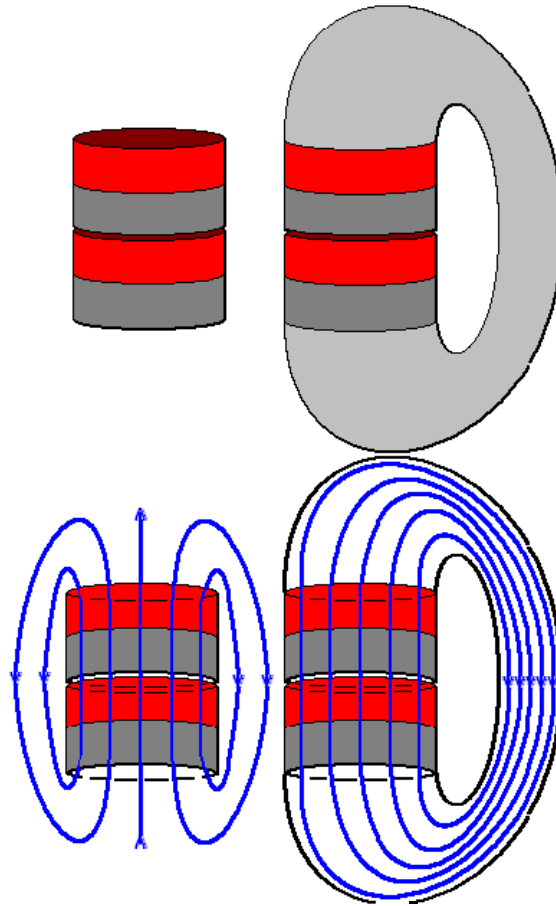
The Mu2e experiment might use a calibration beam of electrons to simulate signal events and study other non-signal possibilities. Due to the potential complexities of backgrounds to the conversion signal, the calibration effort must provide Mu2e with a very detailed description of what might happen during the course of the experiment. This will allow signal events to be distinguished with confidence from background.

Two tools were developed to evaluate a momentum-selection spectrometer that would follow the calibration beam's electron source. The first tool maps out an accurate magnetic field due to currents and magnetic materials. Several mapping techniques were explored, which included Biot-Savart Law calculations, MATLAB numerical integration, equivalent magnetic charge distributions, and series approximations using Legendre polynomials. The second tool plots the trajectory of an electron incident upon the spectrometer using this field map and a fourth-order Runge-Kutta integration based on relativistic mechanics.

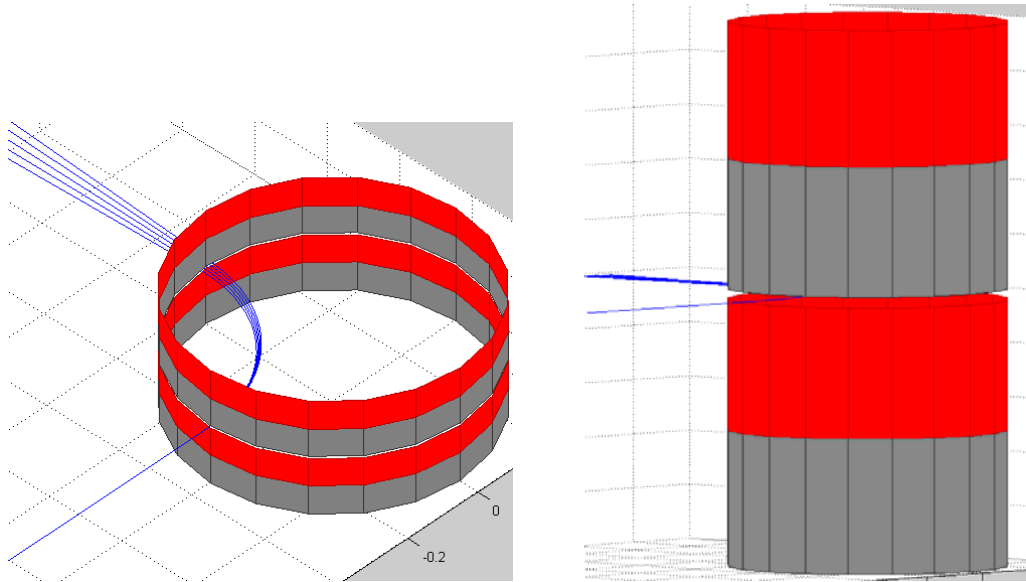
¹ Contact person: George Gollin, g-gollin@illinois.edu, +1 (217) 333-4451.

Spectrometer

The simulated spectrometer consists of two cylindrical, coaxial magnets separated by a 1 centimeter gap. The magnets have a diameter of 70 centimeters and generate a magnetic field of 1 Tesla within the gap capable of bending relativistic electrons. An iron return yoke (at right, in the schematic representation) connects the top and bottom magnets to contain the field lines.



Work this summer has concentrated on designing the specifications of this spectrometer. The spectrometer designs are dependant on the characteristics of the incoming beam (described in detail by Grace Bluhm in another paper) and the way in which the beam reacts to the magnetic fields of the spectrometer magnets. In the ideal case, the spectrometer receives a beam of electrons with narrow spread in entering position and direction of momentum. The profile of the beam exiting the spectrometer differs from that of the incident beam since the electrons have spread out in the plane orthogonal to the spectrometer field. (In our spectrometer 105 MeV/c electrons typically bend through 90°.) Where an electron lies in the beam upon exiting the spectrometer depends primarily on the magnitude of its momentum. Therefore, collimation beyond the spectrometer can remove electrons from the beam with momenta that differ appreciably from the desired nominal momentum of 105 MeV/c.



Magnetic Fields

Magnetic fields are at the heart of selecting the right electrons for a calibration beam. The Lorentz force due to a magnetic field is capable of changing the direction, but not the magnitude of a charged particle's momentum. Furthermore, the amount of acceleration the particle experiences is dependent on that particle's momentum. Therefore, a beam containing some distribution of momenta will diverge when incident upon a magnetic field. If the details of the magnetic field are known, as well as the initial position and direction of the beam, then the final position and direction of a particle with a defined energy is calculable. Collimation beyond the spectrometer will yield a beam of particles with a finely tuned energy.

Defining the magnetic field created by realistic magnets and currents with asymmetric shapes requires a well thought out method. Depending on the source of the field, different modeling strategies were employed:

Biot-Savart Law

Similar to Coulomb's Law for electric fields, the Biot-Savart Law allows a field to be modeled from any collection of current:

$$\vec{B} = \oint \frac{\mu_o}{4\pi} \frac{I \vec{dl} \times \hat{r}}{|\vec{r}|^2} .$$

Even magnetic materials can be modeled in this way as bound currents obey

$$\vec{J}_b = \nabla \times \vec{M} .$$

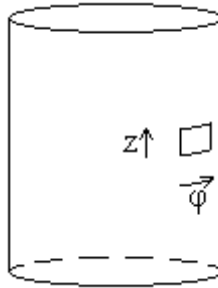
Therefore, an integral can be set up for any distribution of current or magnetic material. Specific to the spectrometer magnets, each with a constant magnetization per unit volume, the bound currents take the form of a surface current in the azimuth direction. Solving these integrals analytically, however, proves to be impossible for all but the simplest current distributions. Numerical integration is a preferred approach for solving these integrals.

Numerical Integration

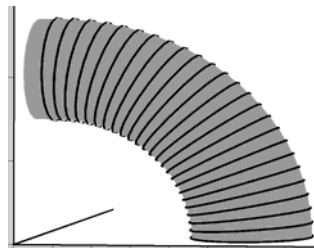
Any integral can be approximated as a sum of discrete terms:

$$\int_a^b f(x)dx = \sum_i^n f\left(i\frac{b-a}{n}\right)\frac{b-a}{n}$$

MATLAB “for loops” can compute these summations to produce magnetic field values, which become more accurate when n is increased. Integrals to compute magnetic fields due to the cylindrical spectrometer magnets employed summations which added up patches of current, illustrated below:



In some experimental circumstances we might want to construct solenoids with more interesting geometries. For example, an electron transport system might consist of curved solenoids that create a sort of magnetic plumbing. Electrons will follow the field lines in helical patterns and around bends in the solenoid piping. For this situation, surface current is not constant as wires bunch and spread out on the inside and outside of curved solenoids. A different approach involved plotting the magnetic field due to a single loop of current, and then using superposition and rotation matrices to build a solenoid out of many loops of current, as indicated schematically in the next figure.



We found that accurate current integrations were difficult to perform in cases when simulated electrons came too close to the current loops comprising the solenoid.

Field maps were plagued with spikes near point currents locations. Computations with n values high enough to eliminate these errors required unreasonable run times.

Magnetic Charge

In some cases, it is possible to define a magnetic charge distribution that is mathematically equivalent to the actual current distribution. Such charge distributions are worth investigating because the Coulomb type field they create gives rise to a scalar potential. Additionally, the magnetic charge distribution may be geometrically appealing. Such is the case for the spectrometer magnets. Certain conditions must be met, however, to allow magnetic charges to be equivalent to current.

The auxiliary field \mathbf{H} is related to the actual magnetic \mathbf{B} by factor of μ_0 in regions free of magnetic material, where the magnetization is zero, such as the gap between the spectrometer magnets:

$$\mathbf{H} \stackrel{\text{def}}{=} \frac{\mathbf{B}}{\mu_0} - \mathbf{M}$$

Furthermore:

$$\nabla \times \mathbf{H} = \mathbf{J}_f$$

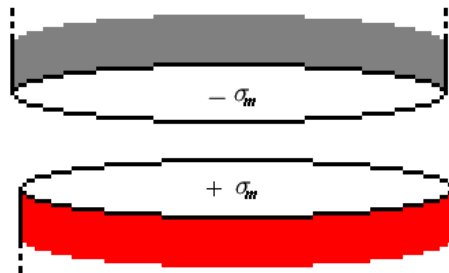
In the absence of free current, the curl of \mathbf{H} is zero, giving rise to a scalar potential of the form:

$$-\nabla \phi = \mathbf{H}$$

Following the mathematical resemblance to polarization in electrostatics, the bound magnetic charge can be calculated from the magnetization:

$$\rho_m = -\nabla \cdot \mathbf{M} \quad \sigma_m = \mathbf{M} \cdot \hat{\mathbf{n}}$$

The divergence of the magnets' constant magnetization is zero, except at the material's boundaries, where the normal dotted with the magnetization yields a constant magnetic charge surface density distribution $-\sigma_m$ and $+\sigma_m$ on the top and bottom pole faces, respectively (see figure, below). The field due to this magnetic charge distribution could be calculated using a numerical integration, but the simple geometry allows us to model the field in a more clever way.

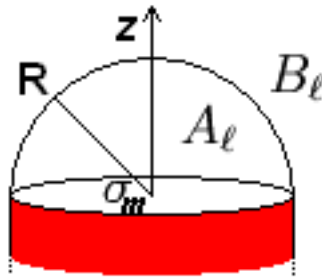


Legendre Polynomials

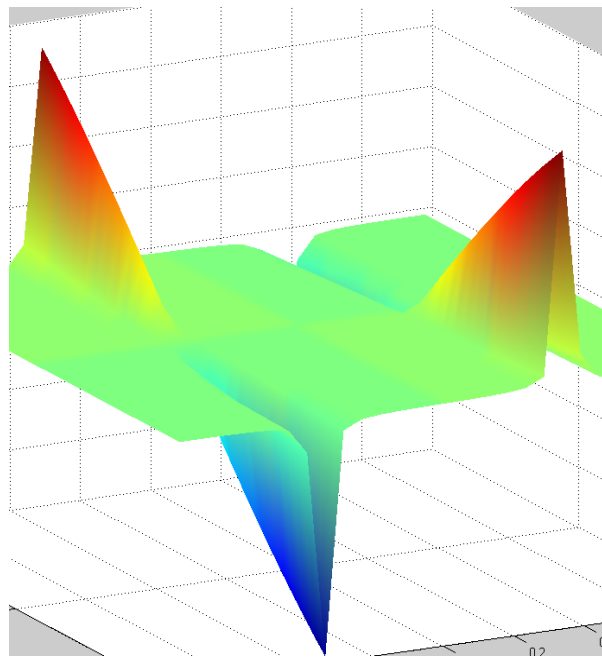
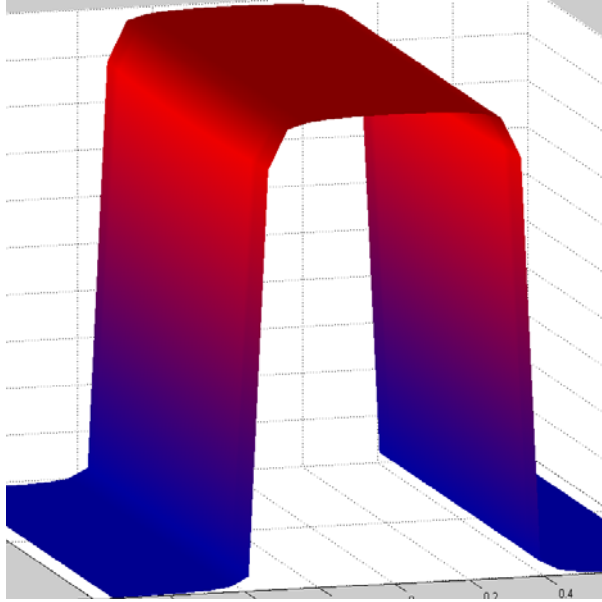
Any axially symmetric function can be expanded as an infinite series of terms which are products of Legendre polynomials and powers of r . The sum is of the form

$$\phi(r, \theta) = \sum_{l=0}^{\infty} \left[A_l r^l + \frac{B_l}{r^{l+1}} \right] P_l(\cos(\theta)).$$

For this task, the potential due to each pole face was calculated independently, and then combined using superposition. The magnetic scalar potential could be defined analytically on the z axis running through the center of the cylindrical spectrometer magnets, and provided the boundary condition necessary to define the A_l and B_l coefficient terms in the series. Also, because the A_l and B_l terms diverge at infinity and at the origin, respectively, space was broken up into two regions. The A_l terms described the potential inside the sphere $r = R$, the radius of the magnet, and the B_l terms described the potential outside of this sphere, illustrated below:



After comparison to previous methods, the field defined by Legendre polynomials was chosen to represent the spectrometer. A plot of the z component of the magnetic field, spanning the region between the top and bottom pole faces, is shown below. Note that the field is roughly constant at its peak, the region inside the magnet radius, and that it drops off sharply outside this region. Below that is a plot of the x component in the same range: $(-.005 < z < .005)$ and $(-.75 < x < .75)$. Note that the field is very close to zero in most regions, and peaks close the edge of each plate indicating that field bulges out of the gap between the magnets slightly. Also note the difference in peak magnitude of the two field directions.



Runge-Kutta Integration

To calculate the trajectory of electrons, Guangyong Koh developed a fourth-order Runge-Kutta integration. The method requires the electron's initial position and momentum information and calls upon a magnetic field generating function to request the field value at each point in the integration. Once complete, the function delivers a matrix containing the electron's position and momentum information at each point in its trajectory. This information was used to determine where and how large exit collimators

will be, as well as what electron parameters will be allowed to pass through these collimators.

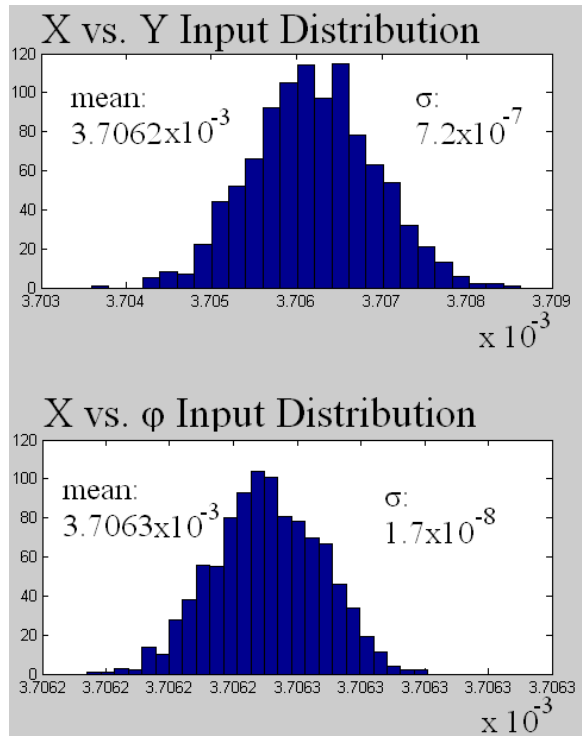
Before any electron trajectory data analysis could be preformed, the Runge-Kutta integration needed to be adequately tuned. This meant determining an appropriate time step size, the time an electron is allowed to move before its momentum information is updated. A step size of 10 picoseconds was chosen because the final position difference between an electron integrated with a step size of 1 picosecond and 10 picoseconds was on the order of 2 nanometers. This resolution is acceptable for now, which is five orders of magnitude smaller than the width of a 100 micron collimator.

Data

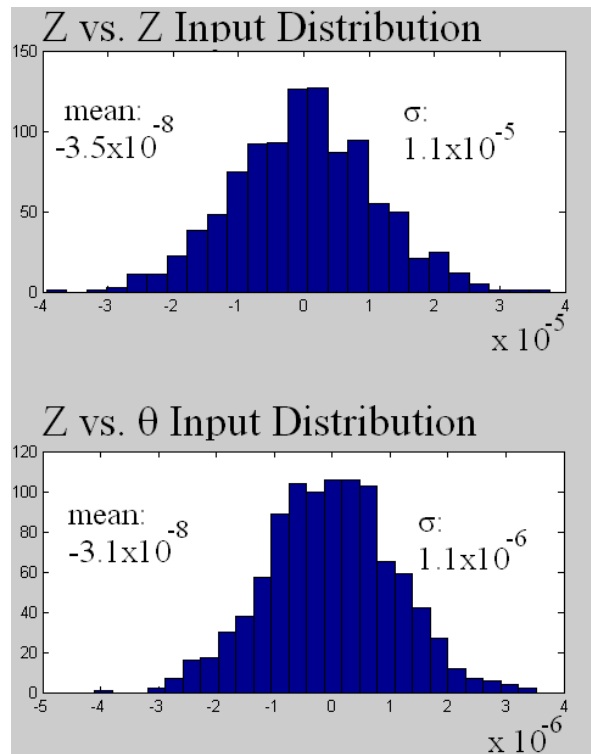
The following table describes the electron input parameters for the spectrometer.

Energy Distribution	105 MeV with 100 keV RMS width
Horizontal Position Distribution	1 micron RMS width
Horizontal Angular Divergence	10 microradians RMS width
Vertical Position Distribution	10 microns RMS width
Vertical Angular Divergence	1 microradian RMS width

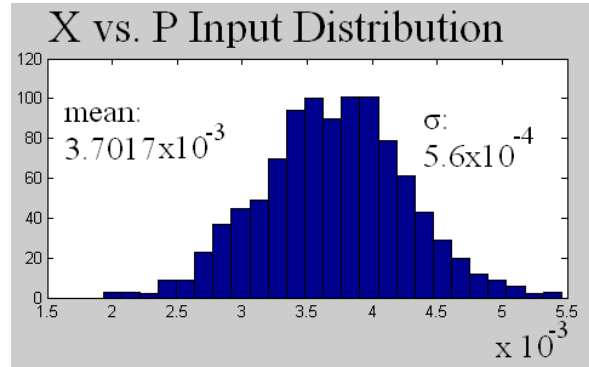
The first set of data consists of five histograms representing the positions of electrons as they cross the plane of a potential collimator for each parameter listed above. Each histogram refers to an individual set of simulations, where only one parameter is varied. These positions were used to estimate the size of an exit collimator.



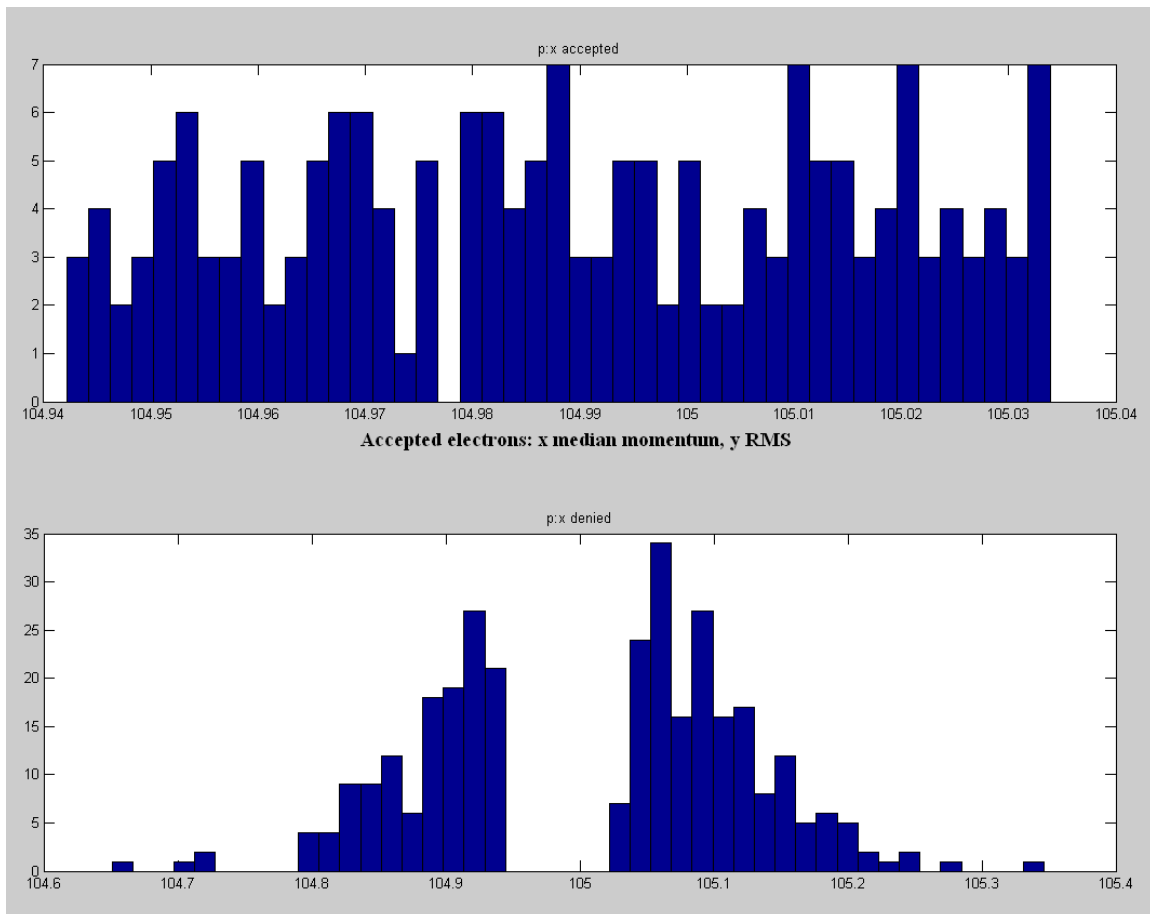
The above histograms illustrate the possible horizontal positions a 105 MeV electron exiting the spectrometer.



The above histograms illustrate the possible vertical displacement a 105 MeV electron exiting the spectrometer. These data suggest a collimator centered at (3.706mm, 0) with a width of 100 microns will allow a sufficient number of 105 MeV electrons to pass.



The above histogram illustrates the possible horizontal displacement of a centered 105 MeV, 100 keV RMS beam and suggests the collimator dimensions estimated above will reduce the beam's energy RMS value.



These final histograms illustrate the accepted (top) and blocked (bottom) electrons, organized by energy. This simulation reveals the realistic behavior of the spectrometer and collimator system, as every parameter was allowed to change. According to this data, the 100 keV RMS beam has been trimmed to about 10 keV RMS.

Conclusion

The spectrometer design in this memo will be a valuable asset to the Mu2e experiment, allowing calibration with electrons with far narrower momentum spread than those taken right from the AØ photoinjector. Additionally, the simulated data generated during the course of the spectrometer research open the door for many more questions which may allow even greater precision and other calibration options:

- Might decreasing the width of the collimator improve the momentum resolution even further?
- How do competing input parameters allow unwanted electrons through the collimator? Might a second collimator several meters downstream eliminate these electrons?
- Do tracks exiting the spectrometer trace back to the spectrometer's center? If so, changing the spectrometer's magnetic field strength may allow a simple way to choose electrons with other momentum.

Acknowledgements

Considerable appreciation goes to the National Science Foundation, the Department of Energy, and the University of Illinois for supporting this research project.

References

- Gollin, George. *Physics 325 and 326: Intermediate Mechanics and Relativity Lecture Notes*. Urbana: University of Illinois, 2009.
- Griffiths, David J. *Introduction to electrodynamics*. 3rd ed. Upper Saddle River, N.J: Prentice Hall, 1999.
- Jackson, John David. *Classical electrodynamics*. 2nd ed. New York: Wiley, 1975.
- Wiss, Jim. *Physics 435: Electromagnetic Fields I*. Urbana: University of Illinois, 2009.